【S-4】

Pathological Study on the Pulmonary Toxicity of Particulate Matters (Carbon Black, Colloidal Silica, Yellow Sands) in Mice

Akinori Shimada

Department of Veterinary Pathology, Tottori University, Tottori-shi, Tottori, Japan

1. Electron Microscopic Study on the Translocation of Ultrafine Carbon Black Particles at the Air Blood Barrier in Lung

Particulate air pollution is associated with cardiovascular morbidity and mortality. Recently, it has been demonstrated that ultrafine particles (UFPs) are able to translocate from the lung into the systemic circulation. Precise mechanisms of the anatomical translocation (crossing the air-blood barrier) of inhaled UFPs at the alveolar wall are not fully understood. In this study, we examined the translocation pathway of the intratracheally instilled ultrafine carbon black (UFCB) from the lung into the blood circulation in mouse. Ultrafine carbon black (UFCB) particles, printex 90 (Degussa, Frankfurt, Germany), the primary diameter of which are 14nm, were instilled to the trachea of 10-week-old ICR female mouse at a concentration of 1mg/0.05ml/body. Lung, regional pulmonary lymph nodes, liver and spleen were removed at 0, 5, 10, 30 min, 1, 2, 6, 12 and 24 hrs after instillation (n = 3 at each time point).Paraffin sections cut at 2μm were processed for Factor VIII-immunohistochemistry to define blood vessels in the alveolar walls. Sections were counter-stained with Hematoxylin. Formalin-fixed lung samples cut into 1-2 mm3 cubes were washed in 1% phosphate buffer, post-fixed with 1% osmium tetroxide, dehydrated in graded alcohol, and embedded in Epon 812. Ultrathin sections were stained with uranyl acetate and lead citrate and examined under TEM-100CX electron microscope (Japan Electron Optical Laboratory, Tokyo).

A small amount of aggregated particle-like materials in the alveolar capillary lumens was occasionally observed in light microscopy. Electron microscopy demonstrated accumulation of intratracheally instilled UFCB in the large-sized pore (gap) formed in the processes of the type I alveolar epithelial cells; occasional invasion of the accumulated UFCB into the denuded basement membrane were observed at the pore. In addition, occasional red blood cells, on which UFCB were attaching, were observed in thecanal of blood vessels at the

alveolar wall with UFCB associated structural changes. These results suggest that inhaled UFPs may, in part, pass the air-blood barrier through the large-sized pore in the type I alveolar epithelial cells.

2. Acute Pulmonary Toxicity Caused by Exposure to Colloidal Silica: Particle Size Dependent Pathological Changes in Mice

To compare the pulmonary toxicity between ultrafine colloidal silica particles (UFCSs) and fine colloidal silica particles (FCSs), mice were intratracheally instilled with 3 mg of 14-nm UFCSs and 230-nm FCSs and pathologically examined from 30 min to 24 hr post-exposure. Histopathologically, lungs exposed to both sizes of particles showed bronchiolar degeneration and necrosis, neutrophilic inflammation in alveoli with alveolar type II cell proliferation and particle-laden alveolar macrophage accumulation. UFCSs, however, induced extensive alveolar hemorrhage compared to FCSs from 30 min onwards. UFCSs also caused more severe bronchiolar epithelial cell necrosis and neutrophil influx in alveoli than FCSs at 12 and 24 hr post-exposure. Laminin positive immunolabellings in basement membranes of bronchioles and alveoli of UFCSs treated animals was weaker than those of FCSs treated animals in all observation times. Electron microscopy demonstrated UFCSs and FCSs on bronchiolar and alveolar wall surface as well as in the cytoplasm of alveolar epithelial cells, alveolar macrophages and neutrophils. Type I alveolar epithelial cell erosion with basement membrane damage in UFCSs treated animals was more severe than those in FCSs treated animals. At 12 and 24 hr post-exposure, bronchiolar epithelial cells in UFCSs treated animals showed more intense vacuolation and necrosis compared to FCSs treated animals. These findings suggest that UFCSs has greater ability to induce lung inflammation and tissue damages than FCSs.

3. Pathological Study on the Pulmonary Toxicity Induced by the Intratracheally Instilled Yellow Sands in Mice

The frequency and volume of yellow sands areincreasing in Japan, resulting in one of the air pollution related threats to human health. There are, however, few reports on the pathological study of the pulmonary toxicity induced by yellow sands. In this study, we examined inflammatory changes in the bronchoalveolar lavage fluids (BALF) and lung tissues of mice intratracheally instilled with yellow sands.

0.05ml of distilled water containing 400μg, A800μg, Aand 2.0 mg of yellow sands (CJ-1, General Science Corporation, Japan) were intratracheally instilled to ICR female mice. At each time points of examination (2 hrs, 24 hrs), number of white blood cell counts in BALF was elevated; neutrophils and lymphocytes were increased. Histopathology demonstrated signs of acute inflammation with mild hemorrhage; macrophages and neutrophils were the major inflammatory cells at 2 hrs and 24 hrs after instillation, respectively. In addition, TUNEL positive findings and 8-OHdG immunoreactivity were observed in the alveolar epithelial cells and macrophages, respectively. These results suggest that yellow sands may induce acute pulmonary inflammatory changes associated with DNA damage by reactive oxygen species

Pathology

Full paper

Tiltle "Acute Pulmonary Toxicity Caused by Exposure to Colloidal Silica: Particle Size Dependent Pathological Changes in Mice"

Running head: ACUTE PULMONARY TOXICITY OF COLLOIDAL SILICA

Authors: THEERAYUTH KAEWAMATAWONG, NATSUKO KAWAMURA, MINA OKAJIMA, MASUMI SAWADA, TAKEHITO MORITA, and AKINORI SHIMADA

Address: Department of Veterinary Pathology, Tottori University, Minami 4-101, Koyama, Tottori-shi, Tottori 680-0945, Japan.

Fax: 0857-31-5424

Corresponding Author: Professor Dr. AKINORI SHIMADA

Department of Veterinary Pathology, Tottori University, Minami 4-101, Koyama, Tottori-shi, Tottori 680-0945, Japan.

E-mail: aki@muses.tottori-u.ac.jp

ABSTRACT

To compare the pulmonary toxicity between ultrafine colloidal silica particles (UFCSs) and fine colloidal silica particles (FCSs), mice were intratracheally instilled with 3 mg of 14-nm UFCSs and 230-nm FCSs and pathologically examined from 30 min to 24 hr post-exposure. Histopathologically, lungs exposed to both sizes of particles showed bronchiolar degeneration and necrosis, neutrophilic inflammation in alveoli with alveolar type II cell proliferation and particle-laden alveolar macrophage accumulation. UFCSs, however, induced extensive alveolar hemorrhage compared to FCSs from 30 min onwards. UFCSs also caused more severe bronchiolar epithelial cell necrosis and neutrophil influx in alveoli than FCSs at 12 and 24 hr post-exposure. Laminin positive immunolabellings in basement membranes of bronchioles and alveoli of UFCSs treated animals was weaker than those of FCSs treated animals in all observation times. Electron microscopy demonstrated UFCSs and FCSs on bronchiolar and alveolar wall surface as well as in the cytoplasm of alveolar epithelial cells, alveolar macrophages and neutrophils. Type I alveolar epithelial cell erosion with basement membrane damage in UFCSs treated animals was more severe than those in FCSs treated animals. At 12 and 24 hr post-exposure, bronchiolar epithelial cells in UFCSs treated animals showed more intense vacuolation and necrosis compared to FCSs treated animals. These findings suggest that UFCSs has greater ability to induce lung inflammation and tissue damages than FCSs.

Keywords : acute pulmonary toxicity, colloidal silica, fine, mice, ultrafine.

INTRODUCTION

Amorphous silica is a naturally occurring or synthetically produced oxide of silicon characterized by the absence of pronounced crystalline structure, and which has no sharp peaks in its X-ray diffraction pattern [33]. There are several types of amorphous silica including fumed silica, colloidal silica, diatomaceous earth and precipitated silica. A number of studies have reviewed the adverse effects of amorphous silica; this silica has potential to induce transient pulmonary inflammation but changes may regress during the recovery period compared to persistent pulmonary inflammation by crystalline silica [26, 29, 35]. In humans, an epidemiologic investigation in occupational exposure to amorphous silica generally showed no evidence of silicotic effect and any potential for carcinogenicity [21]. However, in an occupational setting study, a significant decrease in lung function was observed after amorphous silica exposure [5].

Colloidal silica is one of synthetically amorphous silica that consists of stable dispersion spherical silica particles. The particle sizes are usually of the order from 10 micrometers to less than 10 nanometers. Recently, the colloidal silica became widely used in many industries and available for various applications such as fiber, sizing, diazo paper's manufactures, cellophane film, ceramics, grass fiber, paints, batteries, food and polishing. Toxicological characteristics of the colloidal silica are characterized fairly well as being less toxic than crystalline forms in experimental animals. Kelly and Lee [14] reported that inhalation of 50 or 150 mg/m^3 Ludox colloidal silica for 4 weeks produced dose-related pulmonary effects characterized by accumulation of silica-dust-laden alveolar macrophages, neutrophilic infiltration, and Type II epithelial cell hyperplasia. The severity

and incidence of pulmonary lesions were reduced after a 3-month recovery period, most particle-laden alveolar macrophages (AMs) had disappeared and the remaining AMs were aggregated and sharply demarcated, although small number of silicotic lesions were described and lymph nodes were enlarged. They concluded the no-observable-effect level (NOEL) was 10 mg/m^3. Traditional inhalation toxicity study clearly demonstrated that Ludox colloidal silica is far less active in producing pulmonary effects when compared to Minusil crystalline silica [35]. Moreover most of the biochemical parameters such as lactate dehydrogenase, total protein and N-acetyl glucosaminidase (NAG) returned to control values after a 3- month recovery period. In a subchronic inhalation study of Ludox colloidal silica, Lee and Kelly [16] demonstrated the evidence of the transmigration of particle-laden alveolar macrophage from the alveoli to the interstitium and the tracheo-bronchial lymph node (TBLN) via interstitial lymphatics. In addition, subsequent intra-alveolar silicotic granuloma formations in the interstitium were also observed in the study.

Ultrafine particles (UFP) are commonly defined as particles with diameter less than 100 nm that are ubiquitous in urban ambient air as both singlet and aggregated particles. Ultrafine particulates represent a substantial component in terms of particle numbers in PM_{10} (particulate matter < 10 μm aerodynamic diameter), although they represent a relatively small fraction of the total mass. Currently, the potentially harmful role of ultrafine particle, receives considerable attention as a possible explanation for the epidemiological associations of increase in PM_{10} with health effects [7]. Many toxicological studies makes it clear that ultrafine particles of various types can cause lung inflammatory responses, epithelial cell hyperplasia, inhibit phagocytosis, increased

chemokine expression, lung fibrosis, increased oxidant-generating abilities, and lung tumors [2, 6, 36, 37, 38]. Ultrafine particles are also implicated as of the adverse effects of particulate air pollution on the cardiovascular system by the induction of airway inflammation, leukocyte expression, increased endothelial adhesion molecule in blood, change in blood coagulability and alteration of cardiac electrical activity [8, 9, 12, 23]. It has been demonstrated that ultrafine particles cause greater inflammatory responses and the development of particle-mediated lung diseases than the fine particles per given mass [17, 24].

Data of the pulmonary pathological effects of amorphous colloidal silica in experimental animals are limited and precise mechanisms of the induced pathological changes are not clearly understood. To date, there is no pathological report on comparative pulmonary toxicity of fine and ultrafine colloidal silica. The purpose of this study is to describe acute pulmonary pathological effects caused by intratracheal exposure to amorphous colloidal silica and compare the size effects in light and electron microscopy.

MATERIALS AND METHODS

Experimental animal

Female ICR mice, weighing 28-34 g and at 10-12 weeks of age were purchased from Clear Japan, Inc. (Tokyo, Japan). The mice were housed in an animal facility under 12/12 hr light/dark cycle, temperature of 24 ± 1 °C, relative humidity of 55 ± 10% and negative atmospheric pressure. They were provided with mouse chow and filtered tap water *ad libitum* throughout the experiment. All animal experiments were performed according to the National Institute for Environmental Studies guidelines for animal welfare.

Particles

Ultrafine colloidal silica (Grade PL-1) was obtained as a gift from Fuso Chemical Co., Ltd., Japan. and had a primary particle diameter of 14 nm (Lot No. R2Z007).The silica particles were suspended in water to a concentration of 120 mg/ml.

Fine colloidal silica (Grade PL-20) was also supplied by the same company and had a primary particle size of 213 nm (Lot No. Y1Y001). The particles were suspended in water to a concentration of 239 mg/ml.

Experimental design

45 mice were randomly divided into five control and ten exposure groups of 3 animals each. Ten exposure groups were exposed to 50 μl aqueous suspensions of 3 mg of ultrafine and fine colloidal silica in Milli-Q® purified water by intratracheal instillation. The control groups of mice were instilled to 50μl of Milli-Q® purified water. Animals in each group were sacrificed at 30 min, 2,

6, 12 and 24 hr after instillation.

Histopathology

After gross examination of respiratory organs such as lungs and hilar lymph nodes, the lungs and trachea were removed *en bloc* and instilled with 10% buffered neutral formalin. Whole lungs and hilar lymph nodes were processed according to routine histological techniques. After paraffin embedding, 3 μm sections were cut and stained with hematoxylin and eosin (H&E) for histopathologic evaluation.

Laminin immunohistochemistry

Tissue sections from lung were immunostained by using avidin-biotin complex (ABC) method, in which labeled Streptavidin biotin (LSAB) kit (DAKO, Glostrup, Denmark) was included. After deparaffinization of the sections, the sections were treated with proteinase K for 30 min at 39 °C. The sections were incubated with 3% H_2O_2 to quench endogenous peroxidase for 15 min at room temperature and then with 10% normal goat serum for 5 min in microwave oven 250 w to inhibit nonspecific reactions. Thereafter the sections were reacted over night at 4 °C with Rabbit anti-laminin monoclonal antibody diluted 1:200 (SIGMA®, DAKO, Glostrup, Denmark). The peroxidase conjugated goat anti-rabbit IgG diluted 1:400 (DAKO, Glostrup, Denmark) was reacted to sections as a secondary antibody in microwave oven 200 w for 7 min. The positive reactions resulted in brown staining with the substrate 3,3'-diaminobenzidine tetrahydrochloride (DAB), and the sections were counterstained with hematoxylin.

Electron microscopy

For transmission electron microscopy, lung tissue samples fixed with 10% buffered neutral formalin were rinsed in 0.1 M phosphate buffer (pH = 7.4), post-fixed in 1% osmium tetroxide, dehydrated with serial alcohol and embedded in epoxy resin. Semithin (1-μm thick) sections were stained with toluidine blue to select and locate areas of interest for electron microscopic examination. Ultrathin sections stained with uranyl acetate and lead citrate were examined with a JEM-100CX electron microscope (JEOL, Tokyo, Japan).

RESULTS

Characteristics of fine and ultrafine colloidal silica

The scanning electron microscopic images of ultrafine (UFCSs) and fine (FCSs) colloidal silica are shown in figure 1A and 1B. Both sizes of colloidal silica particles had a compact and spherical configuration. There was substantial difference in diameter between UFCSs (average size of 14 nm) and FCSs (average size of 213 nm). The surface area, which measured by Brunauer, Emmett and Teller (BET) method, was also much greater for UFCSs than FCSs particles, 194 and 13 m^2/g, respectively. There was also a difference between UFCSs and FCSs in terms of metal composition, but both had very low levels (potassium, aluminium, magnesium < 0.01 ppm; Iron < 0.005 ppm ; data were supplied by Fuso Chemical Co., Ltd., Japan). However, FCSs had a little more of sodium (0.10 ppm) and calcium (0.02 ppm) than UFCSs (sodium = 0.05 and calcium < 0.01).

Clinical and gross findings

In FCSs treated animals, there were no exposure-related clinical signs in any observation time. Some mice in UFCSs treated animals showed a sign of dyspnea and died shortly after instillation (data are not shown). Grossly, instillation of UFCSs and FCSs caused congestion, edema and hemorrhage in lung. The degree of lung hemorrhage in UFCSs was more severe than FCSs treated animals at all observation times. In both UFCSs and FCSs treated animals, tiny pin-head sized white foci were scattered particularly in the pleural surface of lung lobes. At all time points, the hilar lymph nodes from UFCSs and FCSs treated animals were slightly enlarged compared to

the control animals.

Light microscopy

Lungs from control animals instilled with Milli-Q® purified water showed normal bronchiolar and alveolar architectures with occasional mild congestion in the alveoli. By 30 min after instillation of UFCSs and FCSs, the lungs showed increased numbers of neutrophils and macrophages and type II alveolar epithelial cell proliferation in alveoli; degeneration and desquamation of some bronchiolar epithelial cells with squamous metaplasia were also observed. More intense alveolar hemorrhage was observed in the UFCSs treated animals compared to FCSs treated animals (Figure 2A, 2B). The hilar lymph nodes of both UFCSs and FCSs treated animals were slightly enlarged with neutrophil infiltration in subcapsular and medullary sinus. At 2 and 6 hr after instillation, the lesions in the lungs and hilar lymph nodes of both UFCSs and FCSs treated animals were similar to those seen in 30 min post-exposure, but the lung lesions of UFCSs treated animals were more severe than FCSs treated animals. Accumulations of numerous particle-laden alveolar macrophages (AMs) were observed in alveolar regions. The alveolar walls adjacent to particle-laden AMs were slightly thickened with type II alveolar epithelial cell hyperplasia. Lungs of mice killed at 6 hr after UFCSs instillation showed more severe bronchiolar epithelial cell desquamation than those of FCSs treated animals. By 12 hours after instillation, UFCSs caused marked degeneration, squamous metaplasia and necrosis of bronchiolar epithelial cells, whereas FCSs caused mild degenerative effects (Figure 3A, 3B); both UFCSs and FCSs treated animals showed a significant influx of neutrophils scattering around the alveoli that contained particles. At

24 hr post-exposure, UFCSs induced more extensive inflammatory changes than FCSs; marked increase of neutrophils sharply demarcated from the remaining normal alveoli were associated with these changes (Figure 4A, 4B). A number of nodular aggregate of neutrophils and particle-laden AMs were observed in some alveolar regions particularly in perivascular areas adjacent to the bronchioles. The nodular lesions consisted of clumps of free particles, some cell debris and particle-laden AMs, and neutrophils. Severe degeneration and necrosis of bronchiolar epithelial cells were still observed in the UFCSs treated animals.

Laminin immunohistochemistry

In control lung tissues, laminin stainings were expressed as a thin and continuous line in bronchial basement membrane, blood vessel basement membrane, around bronchial gland and along alveolar septa (Figure 5A). Weak and scarcely positive staining was observed in discontinuous pattern along basement membranes of bronchioles and alveoli of mice exposed to UFCSs and FCSs. The basement membranes of the alveoli containing clumps of particles and inflammatory cells showed interruptions with a patchy distribution of the immunoreactivity (Figure 5B, 5C). The positive reaction was weaker in the UFCSs treated animals compared to FCSs treated animals in all observation times especially at 24 hr post-exposure.

Electron microscopy

Morphology and distribution of particles in lungs

Two forms of UFCSs, singlet and aggregate forms, were observed in lung tissues. Almost all of singlet UFCSs were spherical, compact electron-dense particles with diameters approximately

10-14 nm. On the other hand, aggregates (diameter > 100 nm) of UFCSs were dominant which consisted of chains and clusters of UFCSs. The ultrastructural findings of FCSs also appeared as compact, spherical electron-dense particles with diameter approximately 213 nm, but all of FCSs remained separated and showed rarely the agglomerated pattern.

Numerous free particles were observed on the bronchiolar epithelial cell surface and along the apical surface of the plasma membrane of alveoli in both UFCSs and FCSs treated animals even at 24 hr post-exposure. Accumulation of particle-laden AMs was also found in the alveoli and bronchiolar lumens. These particle-laden AMs showed round or polygonal shapes with numerous lysosomes and phagolysosomes containing particles. Instilled particles were also observed in the cytoplasm of neutrophils that were presented around clumps of particles. Many singlet FCSs were seen in type II alveolar epithelial cell cytoplasm, in which some particles were occasionally observed in lamellar bodies. There were a few particles in the cytoplasm of type I alveolar epithelial cells. On the contrary, both singlet and small agglomerated UFCSs were incorporated by both types of alveolar epithelium.

Bronchiolar lesions

Ultrastructural analysis of lungs from UFCSs treated animals revealed significant destructive changes of bronchiolar epithelial cells. Damage to bronchiolar epithelial cells was first observed at 30 min after instillation. The most severe changes, which occurred from 12 to 24 hr after treatment, included swelling of endoplasmic reticulum, necrosis, and sloughing (Figure 6A). Vacuolation and squamous metaplasia of bronchiolar epithelial cells were also observed while the

remaining Clara cells showed many mitochondria, irregular arrangement of smooth endoplasmic reticulum (sER) and remarkable edema in the cytoplasm with a few secretory granules. Damage and dissociation of basement membranes of some bronchioles were also observed. By contrast, bronchiolar epithelial cell lesions in FCSs treated animals were similar but less pronounced as compared with the alterations observed in UFCSs treated animals.

Alveolar lesions

The ultrastructure of the lungs from UFCSs treated animals demonstrated marked pathological changes compared to FCSs treated animals. Type I alveolar epithelial cells had features of considerable damage particularly in the areas apposing to the clump of UFCSs particles. There was evidence of advanced injury to type I alveolar epithelial cells, with necrosis and desquamation leading to direct exposure of interstitial tissue to the alveolar space. Damage and dissociation of basement membranes were also found associated with type I alveolar epithelial cell erosion (Figure 6B). Proliferation of type II alveolar epithelial cells was observed in the alveolar lumen. These cells contained condensed mitochondria with multifocal vacuolar degeneration in the cytoplasm. Moreover, desquamation of type II alveolar cells was occasionally seen in some alveoli. The capillary endothelium of alveolar septa showed features of focal damage with increased numbers of vesicles in their cytoplasm. The vascular lumen displayed numerous neutrophilic granulocytes, which infiltrated through the capillary wall to the area with particle accumulation. The areas of lung parenchyma with neutrophil and alveolar macrophage accumulation showed remarkable damage of alveolar wall structures.

DISCUSSION

Occupational exposure to crystalline silica dust is associated with an increased risk for pulmonary diseases such as silicosis. Numerous studies on the crystalline silica toxicity in experimental animals showed inflammatory effects and following pulmonary fibrosis and pulmonary dysfunction [4, 18, 27]. While the pulmonary toxicity of crystalline silica is widely known, there is limited information regarding the lung toxicity by amorphous silica. Animal inhalation studies with synthetic amorphous silica showed reversible inflammation, granuloma formation and emphysema [21, 22]. Occupational exposure to amorphous silica showed no any relevant potential to induce silicosis. Colloidal silica, one of synthetically made amorphous silica that became widely used in many industries and available for various applications, are known to be far less active in producing pulmonary damage when compared to crystalline silica [34]. Subchronic inhalation toxicity studies on colloidal silica reported that inhalation of Ludox colloidal silica produced dose-related pulmonary effects characterized by accumulations of dust-laden polymorphonuclear cells in alveolar ducts, concomitant with neutrophil infiltration and type II alveolar epithelial cell hyperplasia with small numbers of silicotic lesions. The severity and incidence of pulmonary lesions were reduced after a 3-month recovery period [15]. There are, however, limited data of the acute pulmonary effects after exposure to colloidal silica by intratracheal instillation. To understand acute inflammatory events in the lung following colloidal silica exposure, we exposed mice to UFCSs and FCSs and examined pulmonary changes by histology, immunohistochemistry and electron microscopy at intervals from 30 min to 24 hr

post-exposure.

At 30 min and 2 hr post-exposure, there was the evidence of severe degeneration and necrosis of bronchiolar epithelial cells with clumps of colloidal silica particles on epithelial cell surface, but no evidence of inflammatory reactions around the affected bronchioles. This suggested that colloidal silica has a direct toxic effect on lung epithelial cells and bronchiolar epithelial cells seem to be the first target for colloidal silica toxicity. It is generally accepted that the biological responses to amorphous silica are related to its surface properties. The composition and structure of particle surface functionalities such as hydrophilicity, impurities and specific surface functional group play an important role in the biological responses to silica. Silicon functionalities as well as traces of iron impurities on the silica surface are implicated in free radical release at the surface and in subsurface layers of particles [10, 32]. The specific surface silanol groups (SiOH) of silica are directly involved in both hemolysis [13, 25]. and toxicity to alveolar cells *in vitro* [11, 20]. It appears that the silanol presence is a prerequisite for the attachment of silica particles to the cell membrane and consequent cellular uptake by macrophages and neutrophils. This hypothesis is supported by the study showing that the silanol groups form hydrogen bonds with some sites on the cell membrane [31]. Such hydrogen bonding could facilitate the process of phagocytosis. Furthermore, a specific binding of silanol group to the phosphate groups of DNA was reported [19]. This close proximity between DNA and the active sites of the silica surface would enable the short-lived radicals to induce DNA damage [30].

Numerous experimental studies have shown that ultrafine particles have more ability to

enhance lung injury than fine particles of the same chemical composition; the studies included a number of diverse materials such as cobalt, nickel, carbon black and TiO_2 [1, 2, 39, 40]. To our knowledge, there is no detailed pathological report on the pulmonary toxicity induced by different particle sizes of colloidal silica. In the present study, we compared acute pathological findings of lung between UFCSs and FCSs treated animals. The results showed that instillation of UFCSs induced more severe bronchiolar epithelial cell necrosis and purulent inflammation in alveoli than FCSs at 12 and 24 hr post-exposure. Destruction of bronchiolar and alveolar basement membranes was detected as weak positivity of laminin immunolabellings; the immunopositivity in UFCSs treated animals was weaker than those in the FCSs treated animals. These basement membrane damages were associated with particle accumulation. Concomitant ultrastructural studies confirmed more severe damage including dissociation of basement membranes and erosion of type I alveolar epithelial cell in UFCSs treated animals than FCSs treated animals.

Ultrafine particles have a much greater surface area than fine colloidal silica. Several plausible mechanisms have been proposed for the pathogenesis of the initial pulmonary injury following ultrafine particle exposure. The higher toxicity of ultrafine particles than fine particles may be related to the larger surface area per given mass. Higher surface area of particles can play a role as a carrier for co-pollutants such as gases and chemicals, specifically transition metals that could form a coat on the particle surfaces during their formation [7]. Larger surface areas have also been associated with higher inflammatory responses, probably related to increased reactive oxygen species generation, independent of transition metal exposure. However, results of experimental

studies with ultrafine particles composed of low-toxicity materials such as polystyrene have shown an increased inflammatory response with increased total surface area, without any contribution from other factors such as co-pollutants or transition metals. This suggests that surface area drives inflammation in short term and that ultrafine particles induce a greater changes because of the greater surface area they possess [3]. In addition, it has also been suggested that high numbers of ultrafine particles in the alveolar region may overwhelm the capacity of alveolar macrophages to phagocytoze and allow interaction of particles with epithelial cells, resulting in decreased clearing efficiency of ultrafine particles from the alveoli and leading to epithelial cell injury [28].

In summary, this study showed detailed pathology of severe acute pulmonary inflammation and tissue injury induced by intratracheal instillation of colloidal silica; ultrafine colloidal silica particles induced more severe changes than fine colloidal silica particles. Larger surface area of particles might be an important factor in the induction of lung tissue injury.

ACKNOWLEDGMENTS

The authors thank Ms. E. Kawahara for her excellent assistance in electron microscopy at Tottori University.

REFERENCES

1. Baggs, R.B., Ferin, J. and Oberdorster, G. 1997. Regression of pulmonary lesions produced by inhaled titanium dioxide in rats. Vet. Pathol. **34**: 592-597.

2. Brown, D.M., Stone, V., Findlay, P., MacNee, W., and Donaldson, K. 2000. Increased inflammation and intracellular calcium caused by ultrafine carbon black is independent of transition metals or other soluble components. Occup. Environ. Med. **57**: 685-691.

3. Brown, D.M., Wilson, M.R., MacNee, W., Stone, V. and Donaldson, K. 2001. Size-dependent proinflammatory effects of ultrafine polystylene particles: a role for surface area and oxidative stress in the enhanced activity of ultrafines. Toxicol. Appl. Pharmacol. **175**:191-199.

4. Callis, A.H., Sohnie, P.G., Mandel, G.S., Wiessner, J. and Madel, N.S. 1985. Kinetics of inflammatory and fibrotic pulmonary changes in a murine model of silicosis. J. Lab. Clin. Med. **105**: 547-553.

5. Choudat, D., Frisch, C., Barrat, G., el Kholti, A. and Conso, F. 1990. Occupational exposure to amorphous silica dust and pulmonary function. Br. J. Ind. Med. **47**: 763-6.

6. Donaldson, K. and MacNee, W. 2001. Potential mechanisms of adverse pulmonary and cardiovascular effects of particulate air pollution (PM10). Int. J. Hyg. Environ. Health **203:** 411-415.

7. Donaldson, K., Stone, V., Clouter, A., Renwick, L. and MacNee, W. 2001. Ultrafine particles. Occup. Environ. Med. **58**: 211-216.

8. Donaldson, K. and Stone, V. 2003. Current hypotheses on the mechanisms of toxicity of ultrafine

particles. Ann. Ist. Super. Sanita. **39**: 405-410.

9. Frampton, M.W. 2001. Systemic and cardiovascular effects of airway injury and inflammation: ultrafine particle exposure in humans. Environ. Health Perspect. **109**: 529-532.

10. Fubini, B., Giamello, E., Volante, M. and Bolis, V. 1990. Chemical functionalities at the silica surface determining its reactivity when inhaled. Formation and reactivity of surface radicals. Toxicol. Ind. Health **6**: 571-98.

11. Fubini, B., Zanetti, G., Altilia, S., Tiozzo, R., Lison, D. and Saffiotti, U. 1999. Relationship between surface properties and cellular responses to crystalline silica: studies with heat-treated cristobalite. Chem. Res. Toxicol. **12**: 737-745.

12. Gilmour, P.S., Ziesenis, A., Morrison, E.R., Vickers, M.A., Drost, E.M., Ford, I., Karg, E., Mossa, C., Schroeppel, A. Ferron, G.A., Heyder, J., Greaves, M., MacNee, W. And Donaldson, K. 2004. Pulmonary and systemic effects of short-term inhalation exposure to ultrafine carbon black particles. Toxicol. Appl. Pharmacol. **195**: 35-44.

13. Hemenway, D.R., Absher, M.P., Fubini, B. and Bolis, V. 1993. What is the relationship between hemolytic potential and fibrogenicity of mineral dusts? Arch. Environ. Health **48**: 343-347.

14. Kelly, D.P. and Lee, K.P.1990. Pulmonary response to Ludox colloidal silica inhalation exposure in rats. Toxicologist **10**: 202A.

15. Lee, K.P. and Kelly, D.P. 1992. The pulmonary response and clearance of Ludox colloidal silica after a 4-week inhalation exposure in rats. Fundam. Appl. Toxicol. **19**: 399-410.

16. Lee, K.P. and Kelly, D.P. 1993. Translocation of particle-laden alveolar macrophages and

intra-alveolar granuloma formation in rats exposed to Ludox colloidal amorphous silica by inhalation. Toxicology **77**: 205-222.

17. Li, X.Y., Brown, D., Smith, S., Macnee, W. and Donaldson, K. 1999. Short-term inflammatory responses following intratracheal instillation of fine and ultrafine carbon black in rats. Inhal. Toxicol. **11**: 709-731.

18. Lugano, E.M., Dauber, J.H. and Daniele,R.P. 1982. Acute experimental silicosis. Lung morphology, histology, and macrophage chemotaxin secretion. Am. J. Pathol. **109**: 27-36.

19. Mao, Y., Daniel, L. N., Whittaker, N. and Saffiotti, U. 1994. DNA binding to crystalline silica characterized by Fourier-transform infrared spectroscopy. Environ. Health Perspect. **102**: 165-171.

20. Mao, Y., Daniel, L.N., Knapton A.D., Shi X. and Saffiotti, U. 1995. Protective effects of silanol group binding agents on quartz toxicity to rat lung alveolar cells. Appl. Occup. Environ. Hygiene. **10**: 1132-1137.

21. McLaughlin, J.K., Chow, W.H. and Levy, L.S. 1997. Amorphous silica: a review of health effects from inhalation exposure with particular reference to cancer. Toxicol. Environ. Health. **50**: 553-66.

22. Merget, R., Bauer, T., Küpper, H.U., Philippou, S., Bauer, H. D., Breitstadt, R. and Bruening, T. 2002. Health hazards due to the inhalation of amorphous silica. Arch. Toxicol. **75**: 625-634.

23. Nemmar, A., Hoylaerts, M. F., Hoet, P.H.M., Dinsdale, D., Smith, T., Xu, H., Vermylen, J. and Nemery, B. 2002. Ultrafine particles affect experimental thrombosis in an In vivo hamster

model. Am. J. Respir. Crit. Care Med. **166**: 998–1004.

24. Nemmar, A., Hoylaerts, M. F., Hoet, P.H.M., Vermylen, J. and Nemery, B. 2003. Size effect of intratracheally instilled particles on pulmonary inflammation and vascular thrombosis. Toxicol. App. Pharmacol. **186**: 38–45.

25. Pandurangi, R.S., Seehra, M.S., Razzaboni, B.L. and Bolsaitis, P. 1990. Surface and bulk infrared modes of crystalline and amorphous silica particles: a study of the relation of surface structure to cytotoxicity of respirable silica. Environ. Health Perspect. **86**: 327-336.

26. Pratt, P.C. 1983. Lung dust content and response in guinea pigs inhaling three forms of Silica. Arch. Eviron. Health **38**: 197-204.

27. Reiser, K.M., Hesterberg, T.W., Haschek, W.M. and Last, J.A. 1982. Experimental silicosis Experimental silicosis. I. Acute effects of intratracheally instilled quartz on collagen metabolism and morphologic characteristics of rat lungs. Am. J. Pathol. **107**: 176-185.

28. Renwick, L. C., Donaldson, K. and Clouter, A. 2001. Impairment of alveolar macrophage phagocytosis by ultrafine particles. Toxicol. Appl. Pharmacol. **172**: 119–127.

29. Reuzel, P. G. J., Bruijntjes, J. P., Feron, V. J. and Woutersen, R. A. 1991. Subchronic inhalation toxicity of amorphous silicas and quartz dust in rats. Food. Chem. Toxicol. **29**: 341-354.

30. Saffiotti, U., Daniel, L. N., Mao, Y., Shi, X., Williams, A. O. and Kaighn, M.E. 1994. Mechanisms of carcinogenesis by crystalline silica in relation to oxygen radicals. Environ. Health Perspect. **102**: 159-163.

31. Shi, X.L., Dalal, N.S., Hu, X.N. and Vallyathan, V. 1989. The chemical properties of silica

particle surface in relation to silica-cell interactions. J. Toxicol. Environ. Health **27**: 435-454.

32. Vallyathan, V., Shi, X. L., Dalal, N. S., Irr, W. and Castranova, V. 1988.Generation of free radicals from freshly fractured silica dust. Potential role in acute silica-induced lung injury. Am. Rev. Respir. Dis. **138**: 1213-1219.

33. Van Niekerk, W.C.A., Fourie, M.H. and Mouton, G. 2002. Investigation of crystalline phases in silica fume. SIMRAC project support services. SIM 020601.

34. Warheit, D.B., Carakostas, M.C., Kelly, D.P. and Hartsky, M.A. 1991. Four-week inhalation toxicity study with Ludox colloidal silica in rats: pulmonary cellular responses. Fundam. Appl. Toxicol. **16**: 590-601.

35. Warheit, D.B., McHugh, T.A. and Hartsky, M.A. 1995. Differential pulmonary responses in rats inhaling crystalline, colloidal or amorphous silica dusts. Scand. J. Work Eviron. Health. **21**: 19-21.

36. Warheit, D.B. 2004. Nanoparticles: health impacts?. *Materialstoday* : the DuPont company, DE. **February**: 32-35.

37. Zhang, Q., Kusaka, Y., Sato, K., Mo, Y., Fukuda, M. and Donaldson, K. 1998a. Toxicity of ultrafine nickel particles in lungs after intratracheal instillation. J. Occup. Health **40**: 171–176.

38. Zhang, Q., Kusaka, Y., Sato, K., Nakakuki, K., Kohyama, N. and Donaldson, K. 1998b. Differences in the extent of inflammation caused by intratracheal exposure to three ultrafine metals: role of free radicals. J. Toxicol. Environ. Health **53**: 423-438.

39. Zhang, Q., Kusaka, Y. and Donaldson, K. 2000. Comparative pulmonary responses caused by

exposure to standard cobalt and ultrafine cobalt. J. Occup. Health **42**: 179-184.

40. Zhang, Q., Kusaka, Y., Zhu, X., Sato, K. Mo, Y., Kluz, T. and Donaldson, K. 2003. Comparative toxicity of standard nickel and ultrafine nickel in lung after intratracheal instillation. J. Occup. Health **45**: 23-30.

FIGURE LEGENDS

Figure 1. Scanning electron microscopy of ultrafine (A; bar = 50 nm) and fine (B; bar =-490 nm) colloidal silica particles.

Figure 2. Lung sections from mice sacrificed at 30 min after instillation with 3 mg UFCSs (A) or FCSs (B). UFCSs treated mice show more severe congestion and hemorrhage than those in FCSs treated animals. (A) x 390, (B) x 390.

Figure 3. Light microscopy of the lungs from mice sacrificed at 12 hr after instillation with 3 mg UFCSs (A) or FCSs (B). Marked necrosis and desquamation of bronchiolar epithelial cells in A (arrowheads). Moderate bronchiolar epithelial degeneration with bronchiolar epithelial cell desquamation (solid arrow) is seen in B. Aa = alveolar air space; BL = bronchiolar lumen. (A) x 580, (B) x 580.

Figure 4. Light microscopy of the lungs from mice sacrificed at 24 hr after instillation with 3 mg UFCSs (A) or FCSs (B). Marked infiltration of neutrophils with some inflammatory nodules (N) in alveolar air spaces in A. Moderate neutrophil infiltration with a small inflammatory nodule (N) adjacent to the blood vessel (v) in B. (A) x 190, (B) x 190.

Figure 5. Laminin immunohistochemistry in lungs of mice sacrificed at 24 hr after instillation with Milli-Q® purified water (A) or FCSs (B) or UFCSs (C). Brown faint string-like staining patterns along basement membranes (solid arrow) in A. FCSs (B) and UFCSs (C) treated mice show weakly positive discontinuities in the basement membranes of alveoli; weaker positivity and more discontinuous pattern of alveolar basement membranes are observed in UFCSs treated animals (B)

compared with FCSs treated animals (C). Arrowheads identify type II alveolar epithelial cells and arrows indicate alveolar capillary endothelial cells. c: alveolar capillary lumen. (A) x 580, (B) x 580, (C) x 580.

Figure 6. Transmission electron microscopy of lungs from UFCSs treated mice killed at 12 hr post-exposure. Severe destructive changes of bronchiolar epithelial cells included marked swelling of endoplasmic reticulum (white arrows) and necrosis with dissociation of bronchiolar basement membranes in A. Bar = 1.62 μm. Signs of desquamation (solid arrows) and necrosis of type I alveolar epithelial cells (arrowheads) with basement membrane loss in B. Bar = 212 nm. Aa: alveolar air space; BE: bronchiolar epithelial cell; BL: bronchiolar lumen; BM: basement membrane; ET: alveolar endothelial cell; P: particles; RBC: red blood cell; Type I: type I alveolar epithelial cell.

Figure 1.

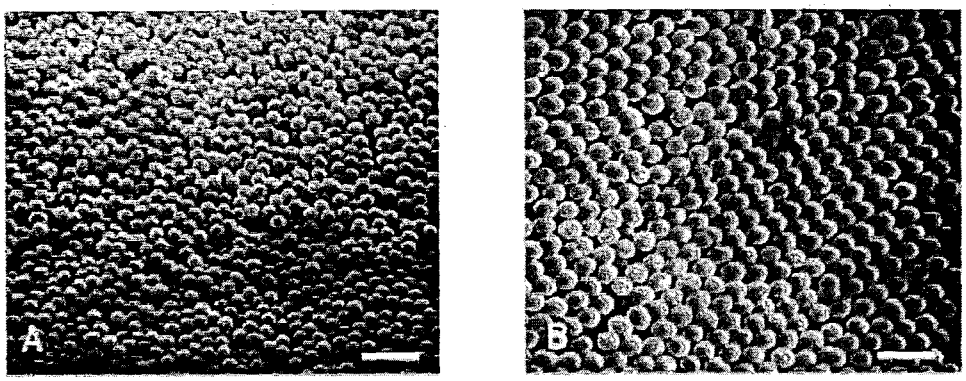

Figure 2.

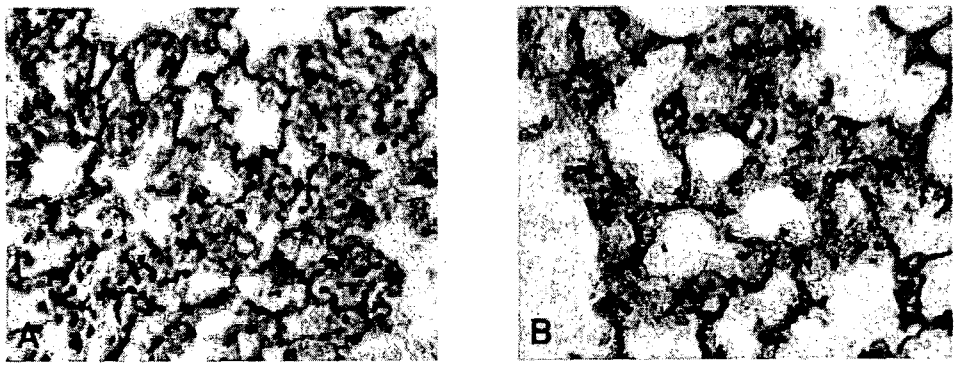

Figure 3.

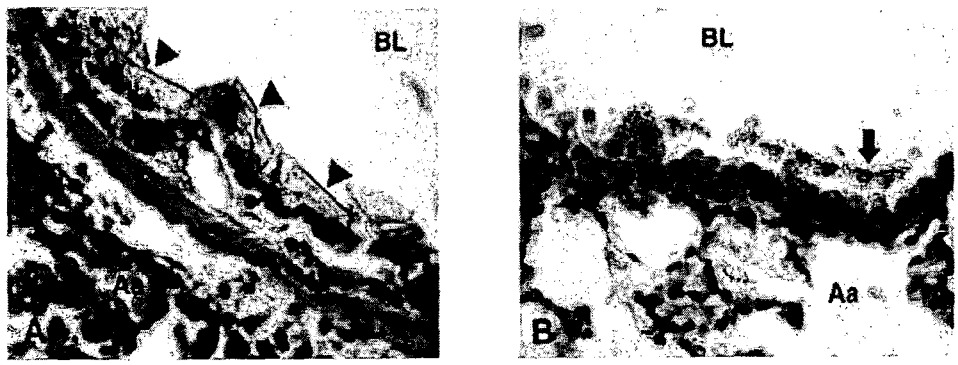

Figure 4.

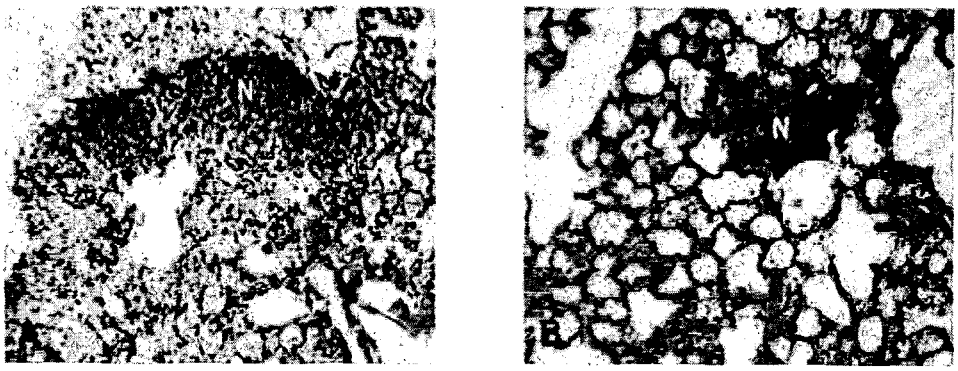

Figure 5.

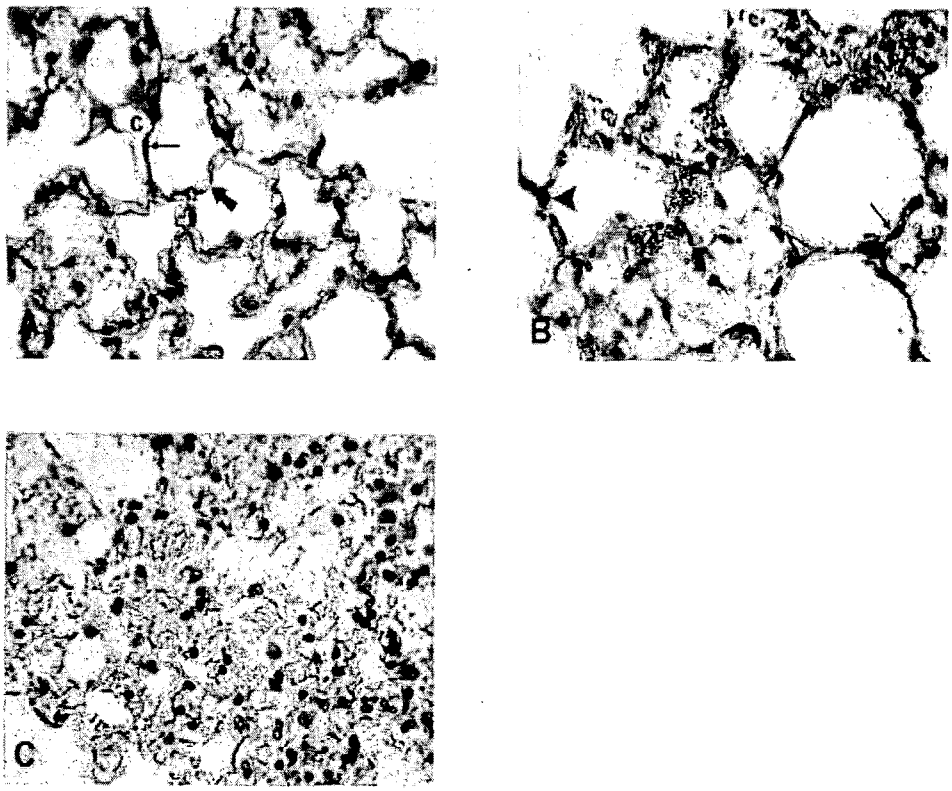

Figure 6.